The EMBO Journal (2007) 26, 3322–3331 | © 2007 European Molecular Biology Organization | All Rights Reserved 0261-4189/07
www.embojournal.org

THE EMBO JOURNAL

Evolution of a bacteriophytochrome from light to redox sensor

Laurie Vuillet[1], Mila Kojadinovic[2], Sébastien Zappa[2], Marianne Jaubert[1], Jean-Marc Adriano[2], Joël Fardoux[1], Laure Hannibal[1], David Pignol[2], André Verméglio[2,3,*] and Eric Giraud[1,3]

[1]Laboratoire des Symbioses Tropicales et Méditerranéennes, IRD, CIRAD, AGRO-M, INRA, UM2, Campus de Baillarguet, Montpellier Cedex, France and [2]CEA Cadarache, DSV/IBEB/SBVME/LBC, UMR 6191 CNRS/CEA/Université Aix-Marseille, Saint-Paul-lez-Durance, France

Bacteriophytochromes are red/far-red photoreceptors that bacteria use to mediate sensory responses to their light environment. Here, we show that the photosynthetic bacterium *Rhodopseudomonas palustris* has two distinct types of bacteriophytochrome-related protein (*Rp*BphP4) depending upon the strain considered. The first type binds the chromophore biliverdin and acts as a light-sensitive kinase, thus behaving as a bona fide bacteriophytochrome. However, in most strains, *Rp*BphP4 does not to bind this chromophore. This loss of light sensing is replaced by a redox-sensing ability coupled to kinase activity. Phylogenetic analysis is consistent with an evolutionary scenario, where a bacteriophytochrome ancestor has adapted from light to redox sensing. Both types of *Rp*BphP4 regulate the synthesis of light harvesting (LH2) complexes according to the light or redox conditions, respectively. They modulate the affinity of a transcription factor binding to the promoter regions of LH2 complex genes by controlling its phosphorylation status. This is the first complete description of a bacteriophytochrome signal transduction pathway involving a two-component system.
The EMBO Journal (2007) **26,** 3322–3331. doi:10.1038/sj.emboj.7601770; Published online 21 June 2007
Subject Categories: signal transduction
Keywords: bacteriophytochrome; light harvesting complexes; redox sensing; *Rhodopseudomonas palustris*

Introduction

Phytochromes are light sensors that were first discovered in plants where they mediate development and growth in response to near infrared light. More recently this class of photoreceptor has also been identified in cyanobacteria (Cphs phytochromes), in proteobacteria (BphPs phytochromes) and in fungi (Fphs phytochromes) (for review see Karniol *et al*, 2005). Most of these chromoproteins use a linear tetrapyrrole chromophore (bilin) and sense red and far-red light via a reversible shift from a red-absorbing form (Pr) to a far-red-absorbing form (Pfr). The discovery of prokaryotic phytochromes has provided new insights into the evolution of phytochromes and has led to a detailed biochemical and structural description of this light sensor family (for review see Rockwell *et al*, 2006).

Bacteriophytochromes (BphPs) have an N-terminal domain homologous to the photosensory core domain (PCD) of plant phytochromes and a C-terminal domain involved in signal transduction. The PCD, which consists of PAS, GAF and PHY sub-domains, autocatalytically binds a linear tetrapyrrole (or bilin) (Karniol *et al*, 2005; Rockwell *et al*, 2006). In most cases, BphPs use the chromophore biliverdin (BV), the simplest linear tetrapyrrole synthesized from heme by a heme oxygenase (Bhoo *et al*, 2001). BV is covalently bound to a Cys residue at the N-terminus of the protein (Lamparter *et al*, 2002). The atomic structure of the region spanning from the N-terminus to the GAF domain of *Dr*BphP from *Deinococcus radiodurans* has recently been determined (Wagner *et al*, 2005); this revealed the key residues that form the BV binding pocket and an unusual trefoil knot that stabilizes the PAS and GAF domains.

In most cases, the BphP C-terminal domain has a two-component histidine kinase motif whose phosphorylation status is dependent on the BphP conformation. The most active phosphorylating state can be either the Pr or the Pfr form, depending on the BphP considered. In some cases, a phosphotransfer to a response regulator (RR), whose gene is often found within the *BphP* operon, has been evidenced (Rockwell *et al*, 2006). Whether or not this phosphotransfer is part of the signaling pathway is still to be demonstrated. A small-angle X-ray scattering solution structure of *Rp*BphP2 from *Rhodopseudomonas* (*Rps.*) *palustris* revealed that a Y-shaped dimer forms through an interaction between the two C-terminal domains. The structure shows how photo-induced signal transduction may stimulate auto-phosphorylation followed by phosphotransfer to a RR (Evans *et al*, 2006).

Besides these common properties, there are interesting differences between BphPs. For the bathyBphPs, the thermal ground state is the Pfr form (Giraud *et al*, 2002; Karniol and Viestra, 2003), whereas for other BphPs, the Pfr form converts to the Pr form in the dark as for plant phytochromes (Butler and Lane, 1965; Lamparter *et al*, 2002). Unlike all BphPs studied so far, *Rp*BphP3 from *Rps. palustris* converts between a Pr form and a Pnr (for *n*ear *r*ed) form, which absorbs at around 645 nm, in a light-reversible way (Giraud *et al*, 2005). The bacteriophytochrome Ppr of the photosynthetic bacterium *Rhodospirillum centenum* is a hybrid of photoactive yellow protein, bacteriophytochrome and histidine kinase domains (Jiang *et al*, 1999). An unusual BphP has also been identified in the photosynthetic bacterium *Bradyrhizobium* ORS278. This BphP binds phycocyanobilin and absorbs light maximally at around

*Corresponding author. SBVME-Laboratoire de Bioénergétique Cellulaire, CEA Cadarache bâtment 156, DSV/IBEB/SBVME/LBC, UMR 6191 CNRS/CEA/Université Aix-Marseille, Saint Paul lez Durance 13108, France. Tel.: +33 44225 4630; Fax: +33 4422 54701;
E-mail: avermeglio@cea.fr
[3]These authors contributed equally to this work

Received: 27 April 2007; accepted: 29 May 2007; published online: 21 June 2007

610 nm in its dark-adapted state (Jaubert *et al*, 2007). This high diversity in BphPs features that most likely reflect their specific *in vivo* functions warrants further study.

In this context, the purple photosynthetic bacterium *Rps. palustris* is a very interesting organism to study. It has a wide distribution and exhibits extraordinary metabolic versatility. Moreover, its photosystem is one of the most elaborate in terms of light harvesting (LH) complexes. In addition to the LH1 complexes that absorb light at around 870 nm and surround the reaction center, peripheral LH2 and LH4 complexes have been described (Tadros and Waterkamp, 1989; Evans *et al*, 1990). The LH2 complexes, which are encoded by three distinct *pucBA* operons (*a*, *b* and *e*), absorb 800 and 850 nm light, while the LH4 complexes, encoded by the *pucBA.d* operon, only absorb at around 800 nm (Evans *et al*, 1990; Hartigan *et al*, 2002). The relative proportion of these LH complexes varies according to environmental factors such as light and oxygen tension (Evans *et al*, 1990; Hartigan *et al*, 2002). Finally, the genomes of five distinct strains of *Rps. palustris* have been sequenced (Larimer *et al*, 2004; http://spider.jgi-psf.org/index.html). The genome of the model strain CGA009 contains six putative *BphP* genes scattered throughout the genome, four of which are close to photosynthesis genes (Larimer *et al*, 2004). The role of these genes has recently been described: (i) *Rp*BphP1 triggers the synthesis of the entire photosynthetic apparatus (Giraud *et al*, 2002, 2004), and (ii) *Rp*BphP2 and *Rp*BphP3 act in tandem to control the expression of the *pucBA.d* operon (Giraud *et al*, 2005). The fourth putative BphP (*Rp*BphP4) gene is in the vicinity of the *pucBA.e* operon, suggesting it could be involved in the control of LH2 complex synthesis. Surprisingly, the *Rp*BphP4 from strain CGA009 does not have the conserved N-terminal Cys residue involved in bilin attachment, and a purified recombinant *Rp*BphP4 homologue isolated from another *Rps. palustris* strain (2.1.6) does not bind any chromophore (Evans *et al*, 2005). Comparison of the CGA009 genome with the genomes of four other *Rps. palustris* strains reveals that this gene is only present in two other strains, BisB5 and HaA2. Unlike *Rp*BphP4s in the CGA009 and 2.1.6 strains, *Rp*BphP4s from BisB5 and HaA2 do have the N-terminal Cys residue responsible for bilin attachment. Can this last form of *Rp*BphP4 capture light? And more generally, how do these different *Rp*BphP4s function and what is their role?

In this study, a phylogenetic analysis of *Rp*BphP4 highlights an organization into two sister clades. By combining biophysical, biochemical and genetic approaches, we demonstrate that *Rp*BphP4 acts either as a bona fide BphP or as a redox sensor depending on the clade. In addition, we show that both types of *Rp*BphP4 use the same signal transduction pathway to control the synthesis of the LH2 complexes.

Results

Phylogenetic analysis of RpBphP4 from Rps. palustris strains

The *RpBphP4* (*rpa1490*) gene of strain CGA009 encodes a protein with the classical bacteriophytochrome architecture (Figure 1B). This gene is flanked by a RR encoding gene (*rpa1489*), and by the *pucBA.e* operon encoding the LH2 complex apoproteins (Figure 1A). To investigate *RpBphP4* gene diversity, polymerase chain reaction (PCR) was used to screen for the presence of this gene in the genome of seven

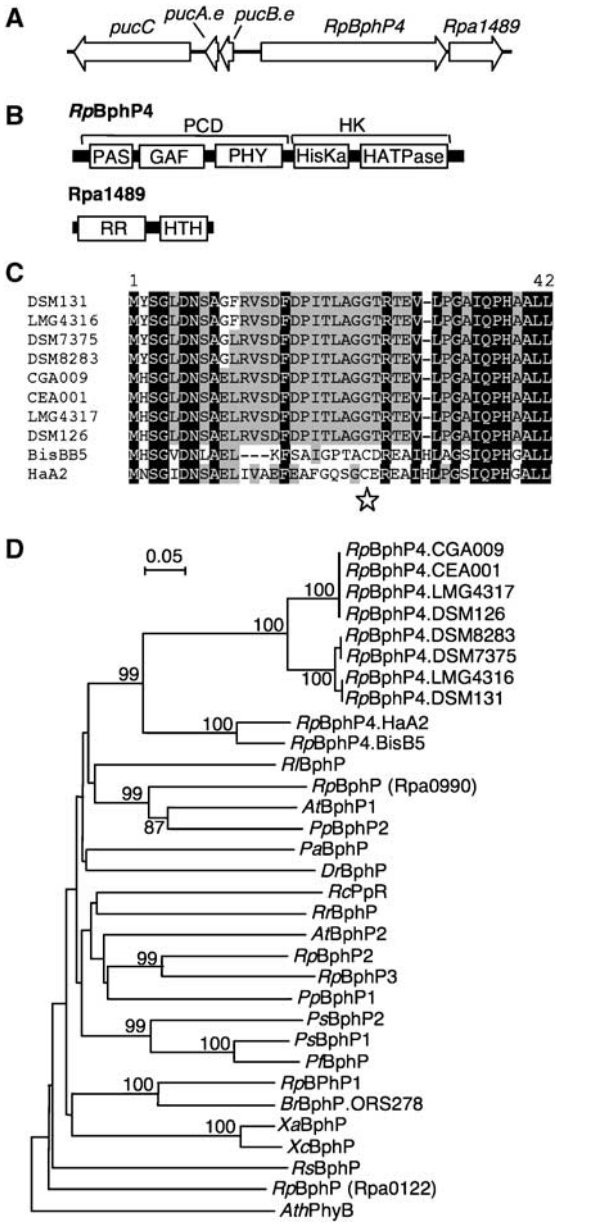

Figure 1 Molecular characterization of *Rp*BphP4. (**A**) Arrangement of genes around *RpBphP4* (*rpa1490* from CGA009). (**B**) Predicted domain structure of *Rp*BphP4 and Rpa1489. PCD: photosensory core domain; HK: histidine kinase domain; HisKa: phosphoacceptor domain; HATPase: ATP binding domain; RR: response regulator domain; HTH: helix–turn–helix domain. (**C**) AA sequence alignment of the N-termini of *Rp*BphP4 proteins from different *Rps. palustris* strains. Residues conserved at more than 50 and 90% are highlighted in gray and black, respectively. Star indicates the Cys residue used as BV binding site. (**D**) Phylogenetic analysis of the BphP family based on an alignment of the GAF domains. The sequences were aligned by CLUSTALX and the tree was generated by the neighbor-joining method and displayed using NJPLOT. Bootstrap values, expressed as percentages of 1000 replications, are shown at the branching points. Species abbreviations: *At*, *Agrobacterium tumefaciens; Ath*, *Arabidopsis thaliana; Br*, *Bradyrhizobium sp.*; *Dr*, *Deinococcus radiodurans*; *Pa*, *Pseudomonas aeruginosa*; *Pf*, *Pseudomonas fluorescens*; *Pp*, *Pseudomonas putida*; *Ps*, *Pseudomonas syringae*; *Rc*, *Rhodospirillum centenum*; *Rl*, *Rhizobium leguminosarum*; *Rp*, *Rhodopseudomonas palustris*; *Rr*, *Rhodospirillum rubrum*; *Rs*, *Rhodobacter sphaeroides*; *Xa*, *Xanthomonas axonopodis*; *Xc*, *Xanthomonas campestris*.

additional *Rps. palustris* strains, using sets of primers specific to the *pucB.e* and *rpa1489* genes, respectively. The *RpBphP4* gene was found in all the strains tested (CEA001, LMG4316, LMG4317, DSM126, DSM131, DSM8283 and DSM7375). The amino-acid (AA) sequences of the newly found *Rp*BphP4s have a very high level of identity (>93%) with *Rp*BphP4 from CGA009, and also lack the canonical Cys residue used as the bilin attachment site (Figure 1C).

A phylogenetic analysis of the GAF domains showed that all *Rp*BphP4s are related to the BphP family and belong to the same monophyletic group, with a very high bootstrap value of 99% (Figure 1D). Similar clustering patterns were obtained using the PHY and PAS domains (data not shown). Interestingly, two sister clades can be distinguished: a large clade containing most of the *Rp*BphP4s, which all lack the conserved Cys residue involved in bilin attachment, and a smaller clade formed by two representatives (HaA2 and BisB5), which have the Cys residue (Figure 1C). The presence or the absence of this canonical Cys residue suggests there are fundamental differences in the physico-chemical properties of *Rp*BphP4s from each clade. In order to confirm such a hypothesis, three *Rp*BphP4s representative of these two clades (CEA001, HaA2 and BisB5) were studied in more detail.

Expression and purification of recombinant RpBphP4 homologues

*Rp*BphP4s from CEA001, HaA2 and BisB5 were coexpressed with a heme oxygenase (required for chromophore synthesis) in *Escherichia coli* and then purified by affinity chromatography. As shown in Figure 2A, the purified recombinant CEA001-*Rp*BphP4 is colorless as is *Rp*BphP4 from the 2.1.6 strain (Evans *et al*, 2005). The absence of bound bilin was confirmed by spectral analysis and zinc-induced fluorescence (Figure 2A). In addition, several attempts of *in vitro* reconstitution by incubation of the purified CEA001-*Rp*BphP4 apoprotein with various bilins (BV, phycocyanobilin and phycoerythrobilin) were unsuccessful to produce a holoprotein. In contrast, *Rp*BphP4s purified from HaA2 and BisB5 are colored and their absorption spectra are characteristic of a bona fide BphP (Figure 2A for HaA2, data not shown for BisB5). Zn-induced fluorescence of proteins separated by SDS–PAGE confirmed the presence of a covalently bound chromophore (Figure 2A).

In an attempt to generate a functional chromophore binding site in CEA001-*Rp*BphP4, a Cys residue was introduced at the conserved position using site-directed mutagenesis (the G24C mutant). We also exchanged the first 33 AA residues with the N-terminal sequence (residues 1–29) of the holoBphP *Rp*BphP1. In both cases, the purified mutated proteins were colorless (data not shown). This implies that the lack of BV binding in CEA001-*Rp*BphP4 is not just due to the absence of the N-terminal Cys but is also the result of additional AA differences. There are possible candidates for this in the chromophore binding pocket of *Dr*BphP (Wagner *et al*, 2005). First, Tyr216, which is involved in hydrogen bonding of the chromophore, is not conserved in the CEA001-*Rp*BphP4 sequence. In addition, four AA (Ile29, Ala212, Phe203 and Met267) out of the 15 involved in Van der Waals' contacts with BV are not conserved. Are these subtle changes sufficient to prevent chromophore binding? Further site-directed mutagenesis and structural studies would be necessary to prove this.

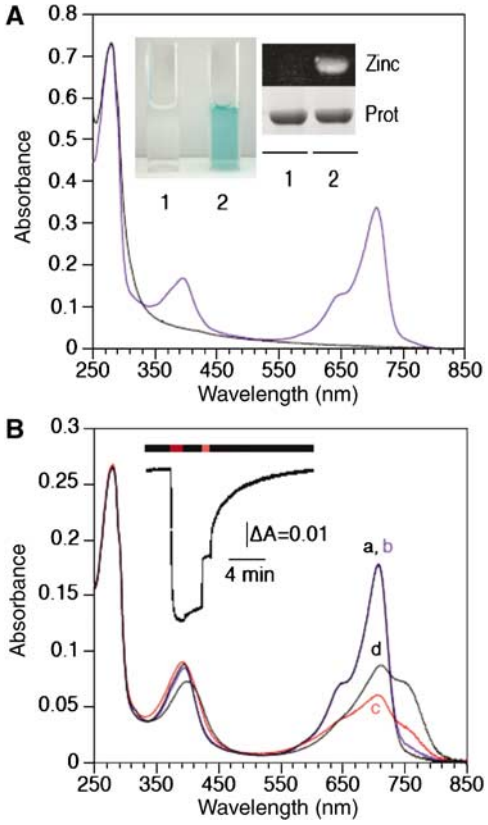

Figure 2 Absorption spectra of *Rp*BphP4 proteins. (**A**) Absorption spectra of recombinant *Rp*BphP4 proteins from strains CEA001 (achromo-*Rp*BphP4, black line) and HaA2 (chromo-*Rp*BphP4, blue line). The inset shows (1) achromo- and (2) chromo-*Rp*BphP4 proteins. The covalent binding of BV to *Rp*BphP4 proteins was visualized by zinc-induced fluorescence or Coomassie staining. (**B**) Absorption spectra of purified HaA2 *Rp*BphP4. The spectra were recorded immediately after: 770 nm illumination (a, black line) followed by 15 min of darkness (b, blue line), 705 nm illumination (c, red line) followed by 15 min of darkness (d, black line). The inset shows the kinetics of changes in absorbance at 750 nm induced by 770 nm light, followed by 2 min of darkness, 1 min of 705 nm light and then a long dark period.

Altogether, these data indicate that there are two distinct types of *Rp*BphP4 in *Rps. palustris*, depending on the strain considered. In most strains, *Rp*BphP4 does not bind BV, whereas the second *Rp*BphP4 type does bind this chromophore. To distinguish between these two *Rp*BphP4 types, the prefixes 'chromo' or 'achromo' (indicating the presence or the absence of a chromophore, respectively) will be used from now onward.

Achromo-RpBphP4 is redox sensitive

When freshly prepared achromo-*Rp*BphP4 from CEA001 is analyzed by non-reducing SDS–PAGE, a major band of around 87 kDa, which corresponds to its expected molecular mass (Figure 3A, lane a) is detected. When the same sample was analyzed after ultrafiltration or dialysis, the 87 kDa band was almost undetectable, although several very high-molecular-weight bands were detected (Figure 3A, lane b). This is likely to reflect the formation of aggregates of an unknown number of subunits. A similar effect was observed when the

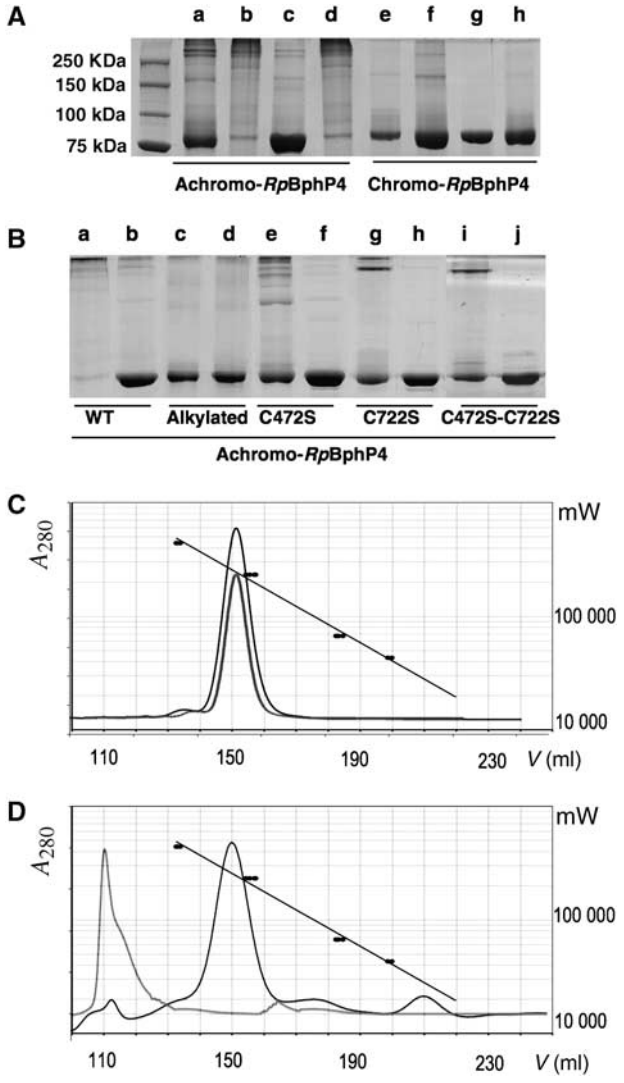

Figure 3 Redox dependence of achromo- and chromo-*Rp*BphP4 proteins. SDS–PAGE analysis and gel filtration of *Rp*BphP4 from CEA001 (achromo) or from HaA2 (chromo) after various treatments. (**A**) Lanes a and e show, respectively, untreated achromo- and chromo-*Rp*BphP4 obtained after nickel affinity chromatography; lanes b and f show the effect of ultrafiltration (Amicon 30 K NMWL); lanes c and g show the effect of 1 mM DTT; and lanes d and h show the effect of 10 mM ferricyanide after reduction by 1 mM DTT. (**B**) Disulfide bond formation in achromo-*Rp*BphP4 (WT), alkylated achromo-*Rp*BphP4, *Rp*BphP4-C472S, *Rp*BphP4-C722S and *Rp*BphP4-C472S-C722S, after oxidation with 1 mM ferricyanide (lanes a, c, e, g and i) or reduction with 1 mM DTT (lanes b, d, f, h and j). (**C, D**) Elution profiles of gel filtration of chromo-*Rp*BphP4 (C) or achromo-*Rp*BphP4 (D) in 50 mM NaCl, 20 mM Tris–HCl pH 8.0 in the absence (gray curves), or in the presence (black curves) of 10 mM DTT. A standard curve is superimposed using the known molecular masses of four protein standards (black circles).

protein sample was exposed to air overnight (data not shown). We therefore assumed that the oligomerization state of the protein was related to the oxygenation, that is, the redox state of the sample. In support of this hypothesis, incubating the protein for 30 min with a reducing agent (DTT) before SDS–PAGE analysis restored the 87 kDa band, while subsequent treatment with an oxidant (potassium ferricyanide) reinduced the formation of aggregates (Figure 3A, lanes c and d). Therefore, the change in the oligomerization state of achromo-*Rp*BphP4 is reversible and redox sensitive. Such an effect was not observed for chromo-*Rp*BphP4s from HaA2 or BisB5, which mainly appear as a single band of the expected size, irrespective the redox conditions (Figure 3A, lanes e–h; data not shown for BisB5). The redox-dependent oligomerization state of achromo-*Rp*BphP4 in solution was confirmed by size-exclusion chromatography (Figure 3D). Oxidized achromo-*Rp*BphP4 eluted with the void volume of the column (Superdex 200), which corresponds to a molecular mass greater than 500 kDa. However achromo-*Rp*BphP4 in the presence of DTT produced a major elution volume peak corresponding to a molecular mass of 200 kDa. Taking into account the predicted molecular mass of the His-tagged *Rp*BphP4 monomer, we conclude that the reduced protein is folded in solution as a homodimer (Figure 3D). When the native chromo-*Rp*BphP4 from HaA2 was separated by gel filtration, the elution volume obtained did not vary with different redox conditions and corresponded to the dimeric form of the protein (Figure 3C).

Analyzing spectra and AA sequences has not revealed any signature of a putative redox center such as those for hemes or flavins, so the redox sensitivity of achromo-*Rp*BphP4 may be determined by one or more Cys residues, as has been described for many thiol-based redox sensors (Paget and Buttner, 2003). To investigate this, achromo-*Rp*BphP4 pre-reduced with DTT was incubated with 10 mM iodoacetamide to fully thiol-alkylate the protein. This modified sample was analyzed by SDS–PAGE in reducing and non-reducing conditions. As shown in Figure 3B, lanes c and d, thiol-alkylated achromo-*Rp*BphP4 was found to be redox independent, confirming that at least one Cys is involved in redox sensing. The AA sequences of achromo-*Rp*BphP4 proteins contain seven Cys residues, two of which (C472 and C722) are conserved in all the achromo-*Rp*BphP4s. C472 is in the PHY domain, whereas C722 is in the His kinase module. To investigate the role of these two Cys residues in the redox sensitivity of achromo-*Rp*BphP4, the single mutants, C472S and C722S, and the double mutant C472S-C722S were produced. SDS–PAGE analysis (Figure 3B) and gel filtration (Supplementary Figure 1) showed that all three mutated proteins form fewer aggregates under oxidizing conditions, indicating that Cys472 and Cys722 are key residues in the redox-dependent oligomerization changes of achromo-*Rp*BphP4.

The chromo-RpBphP4 protein has unusual photochemical properties

Figure 2B shows the absorption spectra of chromo-*Rp*BphP4 from strain HaA2 after red or far-red illumination and different periods of dark adaptation. Under far-red illumination, chromo-*Rp*BphP4 absorbs maximally at around 708 nm (Figure 2B, spectrum a). This is typical of the Pr form of BphPs. This state is relatively stable in the dark. Only a small increase in absorption is recorded at around 750 nm after dark adaptation (Figure 2B, spectrum b). Starting from this state, illumination with red light induces strong bleaching of the 708 nm band, along with a small increase in absorption around 750 nm (Figure 2B, spectrum c). This state, which has strong similarities with the meta-R states of Agp1 BphP (Borucki *et al*, 2005) and phyA (Eilfeld and Rüdiger, 1985), is relatively unstable and slowly transforms (with a half-life of about 2 min) to a new state in the dark. This new state, characterized by the greater absorption of light at around

750 nm typical of the Pfr form (Figure 2B, spectrum d), is relatively stable in the dark and only partially reverts to the Pr state over several hours (not shown). Conversely, illumination of this state with 770 nm light induces rapid formation of the Pr form (Figure 2B, spectrum a). The light-induced formation of Pr and 'meta-R' states starting from the Pfr state is illustrated in Figure 2B (inset). Very similar results were obtained with chromo-*Rp*BphP4 from strain BisB5 (data not shown). Steady-state excitation and emission fluorescence measurements show that only the Pr state of chromo-*Rp*BphP4 is fluorescent (Supplementary Figure 2).

Chromo- and achromo-RpBphP4s use the same signal transduction pathway

Both chromo- and achromo-*Rp*BphP4s have a C-terminal histidine kinase module (Figure 1B). Regulation of the *in vitro* kinase activity was studied by incubating the proteins in the presence of γ-^{32}P-ATP. The redox conditions significantly affected the autophosphorylation of achromo-*Rp*BphP4 of strain CEA001, which only occurred in its reduced form, that is, the dimeric form (Figure 4A, lanes a–c). Such an effect was not observed for the thiol-alkylated achromo-*Rp*BphP4 (Figure 4A, lanes d–f) or for chromo-*Rp*BphP4 from strain HaA2 (Figure 4B, lanes a–c). In contrast, the phosphorylation state of chromo-*Rp*BphP4 was dependent on the light transition (Figure 4B). Indeed, chromo-*Rp*BphP4 from HaA2 appeared to be maximally phosphorylated in its Pfr form (lane d) or following a 705 nm illumination (Figure 4B, lane f), while transition to the Pr state induced a 60% decrease in the level of phosphorylation (lane e).

The genes for chromo- and achromo-*Rp*BphP4 proteins are both found close to a gene encoding a putative transcription factor (Rpa1489), which consists of an N-terminal RR domain and a C-terminal helix–turn–helix DNA binding domain (Figure 1B). Alignment of the sequences of these putative transcription factors from the CEA001 and HaA2 strains shows they have 92% identity. Efficient phosphotransfer from both types of *Rp*BphP4 to Rpa1489 was observed (Figure 4C). As expected, the level of phosphorylation of Rpa1489 can be correlated to the redox or light conditions depending on the *Rp*BphP4 type. Therefore, both types of *Rp*BphP4 are involved in the same signal transduction pathway that is probably a two-component regulatory system, where the Rpa1489 homologue is the last element.

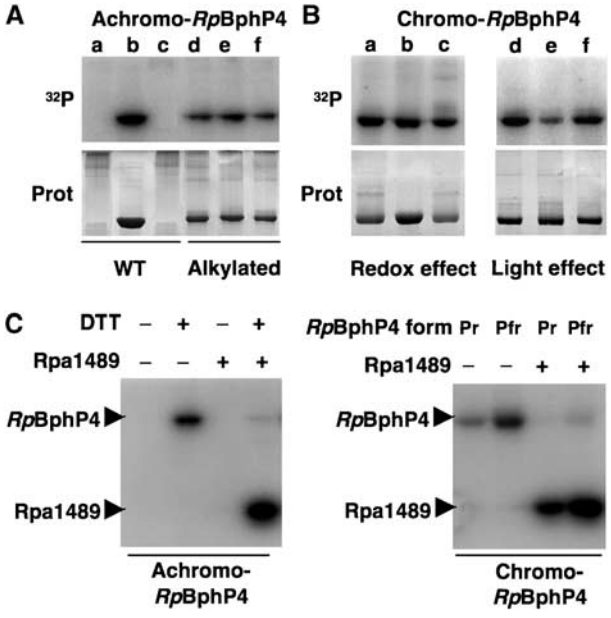

Figure 4 Achromo- and chromo-*Rp*BphP4 proteins act as redox or light-regulated histidine kinases, respectively. (**A**) Effect of redox conditions on the kinase activity of achromo-*Rp*BphP4 (WT) and alkylated achromo-*Rp*BphP4 (alkylated). Lanes a and d, untreated; lanes b and e, reduced with 1 mM DTT; and lanes c and f, oxidized with 1 mM ferricyanide. Proteins were incubated with γ-^{32}P-ATP for 15 min. The reaction products were separated by SDS–PAGE and the gels were autoradiographed (top) or stained with Coomassie blue (bottom). (**B**) Effect of redox or light conditions on the kinase activity of chromo-*Rp*BphP4. For the redox effect, the sample was subjected to 15 min of pre-illumination with 705 nm light followed by 15 min of dark adaptation, and was left untreated (lane a), or treated with 1 mM DTT (lane b) or 1 mM ferricyanide (lane c). For the light effect, chromo-*Rp*BphP4 was converted to its Pfr (lane d), Pr (lane e) or 'meta R' (lane f) forms; the Pfr form was obtained by 15 min of pre-illumination at 705 nm followed by 15 min of dark adaptation, the Pr form by illumination at 770 nm and the 'meta R' form by illumination at 705 nm. (**C**) Phosphotransfer between *Rp*BphP4 and the RR Rpa1489. Transfer of the phosphoryl group between the achromo-*Rp*BphP4 and Rpa1489 relative to the redox conditions (left panel). Phosphotransfer between chromo-*Rp*BphP4 and Rpa1489 relative to the light conditions (right panel).

The transcription factor Rpa1489 binds to pucBA promoters

The position of *RpBphP4/rpa1489* genes in the vicinity of the *pucBA.e* operon suggests that the putative transcription factor Rpa1489 might bind to the *pucBA.e* promoter. DNA binding of recombinant Rpa1489 was first tested by gel mobility shift assays, using the promoter regions of the five *pucBA* operons identified in strain CGA009. The results shown in Figure 5A indicate that Rpa1489 binds specifically to the *pucBA.b* and *pucBA.e* promoters *in vitro*. This specific interaction depends on the phosphorylation state of Rpa1489 (Figure 5B). The affinity of unphosphorylated Rpa1489 for the *pucBA.b* promoter is seven-fold lower than that of phosphorylated Rpa1489. Similar results were obtained for the *pucBA.e* promoter (data not shown).

In addition, we investigated the Rpa1489 DNA binding sites on the *pucBA.b/e* promoters by DNase I protection (footprint). The DNase I digestion patterns (Figure 5C) confirmed that Rpa1489 protects both *pucBA.b* and *pucBA.e* promoters. The sequences of the protected regions are very similar and both contain the palindromic motif TGTCCGN$_8$CGGACA. Interestingly, the *pucBA.b/e* promoters contain a TGTN$_{12}$ACA palindrome downstream and juxtaposed to the Rpa1489 DNA binding site. This sequence corresponds to the DNA binding site of PpsR, a key regulator of photosynthesis gene expression in purple bacteria (Elsen *et al*, 2005). *Rps. palustris* is unusual in having two distinct PpsRs (encoded by *ppsR1* and *ppsR2*) like the photosynthetic *Bradyrhizobium* sp. ORS278 strain (Jaubert *et al*, 2004). We tested whether purified PpsR2 (Giraud *et al*, 2004) binds to the promoters of the *pucBA.b/e* operons. As shown in Figure 5B, PpsR2 binds these promoter regions downstream of the Rpa1489 binding site, strongly suggesting that these two *pucBA* operons are under the control of Rpa1489, PpsR2 and most probably PpsR1.

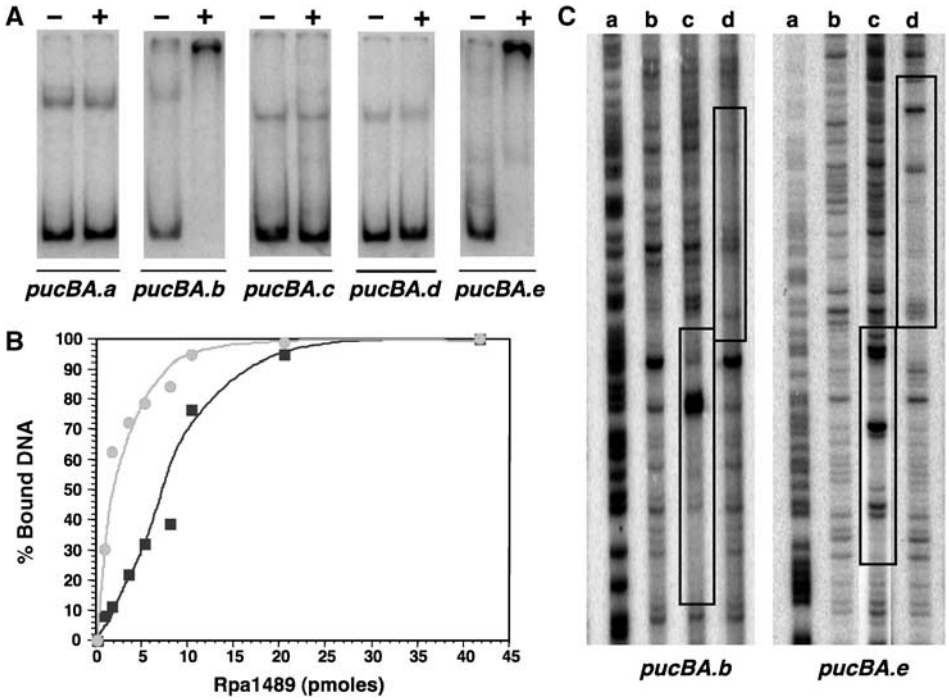

Figure 5 The transcription factor Rpa1489 binds the *pucBA.b/e* promoters. (**A**) Gel mobility shift assays with purified Rpa1489. The left lane (−) of each gel contained only ^{32}P-labeled probe, while the right lane (+) contained in addition 0.5 μM Rpa1489. *PucBA* from *a* to *e* represent the five *pucBA* promoter regions identified in *Rps. palustris* CGA009 strain (Larimer *et al*, 2004). (**B**) Binding affinity of unphosphorylated (blue curve) and phosphorylated (green curve) Rpa1489 to the *pucBA.b* promoter. Phosphorylated and unphosphorylated forms of Rpa1489 were obtained by incubating Rpa1489 with achromo-*Rp*BphP4 for 30 min under reducing conditions in the presence or absence of ATP, respectively. (**C**) DNase I footprints of Rpa1489 and PpsR2 binding to the *pucBA.b/e* promoter regions. G + A ladder (lane a), control without protein (lane b), 1 μM Rpa1489 (lane c), 1 μM PpsR2 (lane d) (for color figure see online version).

Chromo- and achromo-RpBphP4 control LH2 synthesis

The above biochemical data are strong indications that *Rp*BphP4, sensing either a light or a redox signal, may control the synthesis of LH2 complexes through the regulation of some *pucBA* operons using a cognate RR (Rpa1489). The next step was to confirm this role *in vivo*. The photosystem composition of three *Rps. palustris* strains, harboring either achromo- (CEA001) or chromo-*Rp*BphP4 (BisB5 and HaA2), and their corresponding *Rp*BphP4 deletion mutants were analyzed after growth under different light and redox conditions. The absorption spectra of intact cells were recorded at 77 K. At this low temperature, absorption in the near infrared range by LH2 and LH1 complexes can be clearly distinguished, making it more straightforward to calculate the relative contribution made by each type of complex. For BisB5 (chromo-*Rp*BphP4-containing) cells grown in the dark at O_2 tensions of between 1 and 8%, a small amount of photosynthetic apparatus was observed only at 1% (Figure 6A). In contrast, large amounts of photosynthetic apparatus were synthesized when cells were illuminated with 700 or 770 nm light, irrespective of the O_2 tension (Figure 6A, left panel). This effect is related to the activating effect of *Rp*BphP1 (Giraud *et al*, 2002, 2004). Illumination with each of these wavelengths however has a different effect on the synthesis of LH1 and LH2 complexes. The LH2/LH1 ratios are 1 and 0.7 for illumination with 700 or 770 nm light, respectively (Figure 6A). On the other hand, no differential effect of illumination with 700 or 770 nm light on LH2 synthesis was observed for the BisB5Δ*Rp*BphP4 mutant (Figure 6A, right panel). A similar result was observed at 3 or 8% O_2 tension for both the BisB5 and HaA2 strains (not shown). These experiments indicate that 700 nm light absorbed by chromo-*Rp*BphP4 activates the synthesis of LH2 complexes.

A different situation was observed for strain CEA001 (an achromo-*Rp*BphP4 containing strain). A significant amount of photosynthetic apparatus was synthesized in the dark at O_2 tensions lower than 8% (Figure 6B, left panel). In addition, a clear increase in the LH2/LH1 ratio was observed when the O_2 tension decreased from 8 to 1% (Figure 6B, left panel). The deletion of *Rp*BphP4 in strain CEA001 resulted in an approximately two-fold lower LH2/LH1 ratio, but did not affect the amount of LH1 at the various O_2 tensions tested (Figure 6B, right panel). Contrary to the effect observed in BisB5 or HaA2, illumination with 700 nm light induced a decrease in LH2 synthesis, as previously reported (Giraud *et al*, 2005).

Another difference in the behavior of strains CEA001 and BisB5/HaA2 was observed for cells grown under anaerobic conditions under white light. CEA001 cells synthesized many more LH2 complexes than the BisB5 and HaA2 strains (data not shown). On the one hand, this is consistent with the activation of CEA001 achromo-*Rp*BphP4 under reducing conditions, and on the other, with the inability to synthesize the chromophore of BisB5/HaA2 chromo-*Rp*BphP4 in the absence of O_2.

Altogether these data, summarized in Figure 6C, indicate that both achromo- and chromo-*Rp*BphP4s play an activating role in the synthesis of LH2 at low O_2 tension or under specific light wavelengths, respectively. The conditions of

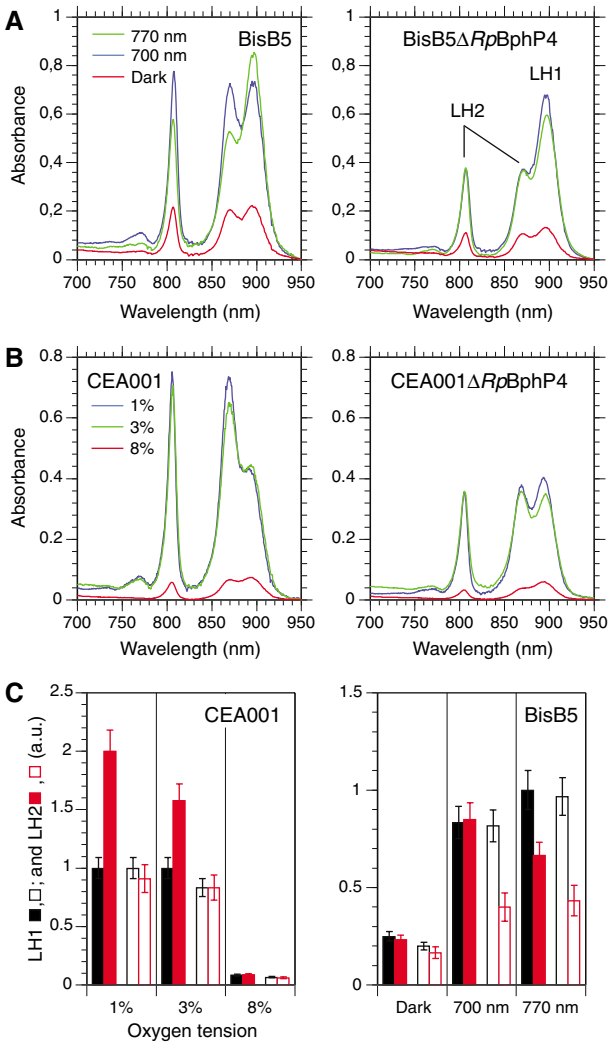

Figure 6 Effect of light and oxygen tension on the synthesis of the photosynthetic apparatus in WT and *Rp*BphP4 deletion mutants. (**A**) Left panel, absorption spectra recorded at 77 K of intact BisB5 cells grown at 1% oxygen tension in the dark (red spectrum), or with 700 nm (blue spectrum), or 770 nm (green spectrum) light. Right panel, as for the left panel, but for the BisB5Δ*Rp*BphP4 mutant. (**B**) Left panel, absorption spectra recorded at 77 K of intact CEA001 cells grown in the dark at 1% (blue spectrum), 3% (green spectrum) and 8% (red spectrum) oxygen tension. Right panel, as for the left panel, but for the CEA001Δ*Rp*BphP4 mutant. (**C**) Left panel, amounts in arbitrary units of LH1 (black bars) and LH2 (red bars) synthesized in the dark in strain CEA001 (filled bars) and mutant CEA001Δ*Rp*BphP4 (open bars) as a function of the oxygen tension. Right panel, amounts of LH1 (black bars) and LH2 (red bars) synthesized in the dark or under 700 or 770 nm illumination in strain BisB5 (filled bars) and mutant BisB5Δ*Rp*BphP4 (open bars). All cell cultures were at 1% oxygen tension.

this induction are consistent with their respective kinase activities described above.

Discussion

Evolution of RpBphP4 from a light to a redox sensor

Rps. palustris is known as one of the most energetically versatile microorganisms, as it is able to grow under different environmental conditions by using photosynthesis, aerobic or anaerobic respiration, or fermentation. To rapidly adapt its metabolism to changes in oxygen or light availability, *Rps. palustris* uses a set of sensors like PpsRs and BphPs.

In this study, we show that there is an additional level of regulation of LH2 complex synthesis by the sensor *Rp*BphP4. Depending on the strain considered, *Rp*BphP4 responds to either redox or light signals to activate synthesis of LH2 complexes. Light- and redox-sensing *Rp*BphP4 proteins, chromo- and achromo-*Rp*BphP4, respectively, correspond to two versions of the same protein, found in the same synthon of different *Rps. palustris* strains. They form two sister clades phylogenetically related to the phytochrome family, suggesting that a BphP ancestor could have evolved from a light sensor to a redox sensor in some of the *Rps. palustris* strains studied. To our knowledge this is the first description of evolution in the nature of signal perception by a histidine kinase sensor. The loss and acquisition of specific Cys residues would thus be decisive events in modifying the sensory properties of *Rp*BphP4; the canonical N-terminal Cys used as the chromophore binding site in all BphPs is specific to chromo-*Rp*BphP4 while Cys422 and Cys722 are specific to the redox-sensing achromo-*Rp*BphP4.

Among the 10 strains of *Rps. palustris*, which have *Rp*BphP4, only two have a chromo-*Rp*BphP4. Interestingly, all the achromo-*Rp*BphP4s were found in collection strains, while the two chromo-*Rp*BphP4 are from strains recently isolated from the environment. However, given the very high similarity between the different achromo-*Rp*BphP4 sequences, it is very unlikely that the same AA modifications have occurred in different laboratories. As already mentioned, *Rps. palustris* strains with achromo-*Rp*BphP4 contain more LH2 complexes than those containing chromo-*Rp*BphP4, when grown under anaerobic conditions in the light, the standard conditions for selecting anoxygenic photosynthetic bacteria. These strains are highly pigmented due to the large quantity of LH2 complexes. When isolating photosynthetic bacteria, selection may be biased toward the more strongly colored colonies, and this may explain the large number of achromo-*Rp*BphP4 strains found in laboratory collections.

Achromo-RpBphP4, a redox sensor

The *in vivo* phenotypes of deletion mutants indicate that achromo-*Rp*BphP4 is a redox-dependent activator of LH2 synthesis. *In vitro* analyses suggest that this redox sensing is mediated by two conserved Cys residues, Cys422 and Cys722, located in the PHY and in the His kinase domains, respectively. These two Cys are involved in the reversible redox-dependent formation of aggregates via intermolecular disulfide bonds. This change of oligomerization state can be correlated to the kinase activity of the protein, which is only active in its dimeric form. This is in agreement with previous studies, which showed that histidine kinases of two-component systems always act as dimers where the subunits trans-phosphorylate each other (Yang and Inouye, 1991; Ninfa *et al*, 1993).

In the absence of a complete structural description of a classical BphP, including both the PHY and histidine kinase domains, it is not possible to fully explain the role of these cysteines in the oligomerization of the protein. However, the involvement of redox-active cysteines in modulating the activity of regulators of photosystem synthesis has already been proven in purple bacteria. For example, an

intramolecular disulfide bond, mediated by oxygen, enhances the DNA binding activity of CrtJ, the aerobic repressor of photosynthetic apparatus synthesis in *Rhodobacter capsulatus* (Masuda *et al*, 2002). In contrast, PpsR1, the counterpart transcription factor in *Bradyrhizobium* has only one Cys residue and can form an intermolecular disulfide bond. This leads to a switch from a tetrameric to an octameric form when the redox potential increases (Jaubert *et al*, 2004). Regulation by intermolecular disulfide bonds has also been demonstrated for the global regulator RegB. RegB and its cognate RR RegA control a large number of oxygen response processes (Elsen *et al*, 2004). Thanks to the essential role of a metal cofactor, the formation of an intermolecular disulfide bond modulates the oligomerization state from a tetramer under oxidizing conditions to a dimer under reducing conditions. This intermolecular bond also affects RegB autophosphorylation, which can only autophosphorylate in its dimeric form (Swem *et al*, 2003). The changes in oligomerization state observed *in vitro* for *Rp*BphP4 are probably related to the mechanisms described above.

Chromo-RpBphP4, an atypical light sensor

We show that chromo-*Rp*BphP4 has unusual spectral properties, with significant bleaching of the Pr form when illuminated with a small concomitant increase in absorption in the near infrared region (Figure 2B). This is probably a consequence of a very slow conversion from the intermediate meta-R state to the stable Pfr state. In fact, this unusual property is consistent with the light regulation of photosynthetic apparatus synthesis in *Rps. palustris*. Indeed, the synthesis of the photosystem and its associated pigments is activated by the Pr state of *Rp*BphP1, that is, with 770 nm illumination (Giraud *et al*, 2002, 2004). In contrast, we show in this study that the synthesis of LH2 is activated by 700 nm light, that is, via both the 'meta-R' and the Pfr states of chromo-*Rp*BphP4. In other words, LH2 synthesis in strains BisB5 or HaA2 requires both 770 and 700 nm light. Such light conditions would yield a mixture of both Pr and Pfr states for a classical BphP. However, due to its poor absorption of near infrared light, chromo-*Rp*BphP4 is preferentially in its activated 'meta-R' state when excited by both 700 and 770 nm light (Supplementary Figure 3).

RpBphP4, the first element in a two-component system

Our data show that both chromo- and achromo-*Rp*BphP4s have a kinase activity regulated by light or redox conditions, respectively. Both phosphorylate a transcription factor homologous to Rpa1489, increasing its binding affinity for the promoter regions of the *pucBA.b/e* operons. The enhancement of LH2 synthesis at low oxygen tensions for CEA001 (achromo-*Rp*BphP4) or in 700 nm light for BisB5 and HaA2 (chromo-*Rp*BphP4) implies that the Rpa1489 homologues activate the transcription of both *pucBA* operons under their phosphorylated form. Such regulation is also suggested by the phenotype of *Rp*BphP4 deletion mutants, which are strongly affected in LH2 synthesis. Altogether, this describes a complete two-component signaling pathway to control LH2 synthesis initiated by a BphP sensing either light or oxygen.

The presence of a PpsR binding motif immediately downstream of the DNA binding site of Rpa1489 indicates, however, that additional regulators (PpsR1 and PpsR2) could be involved in LH2 synthesis (Figure 7). We show that PpsR2 binds to *pucBA.b/e* promoters (Figure 5C). This transcription factor represses the synthesis of the entire photosynthetic apparatus, including the LH chromophores. This repressive effect is antagonized by far-red light via *Rp*BphP1 (Giraud *et al*, 2004). Similarly, LH2 synthesis is strongly repressed in a PpsR1 mutant, showing that this transcription factor also acts as a regulator of the expression of *pucBA* genes (Supplementary Figure 4).

In conclusion, the control of photosystem synthesis in *Rps. palustris* is highly sophisticated and involves a complex network of different light and redox regulatory pathways. This complexity, coupled with the sensor flexibility, enables this species to adapt precisely to different environments and to rapid changes in light and redox conditions.

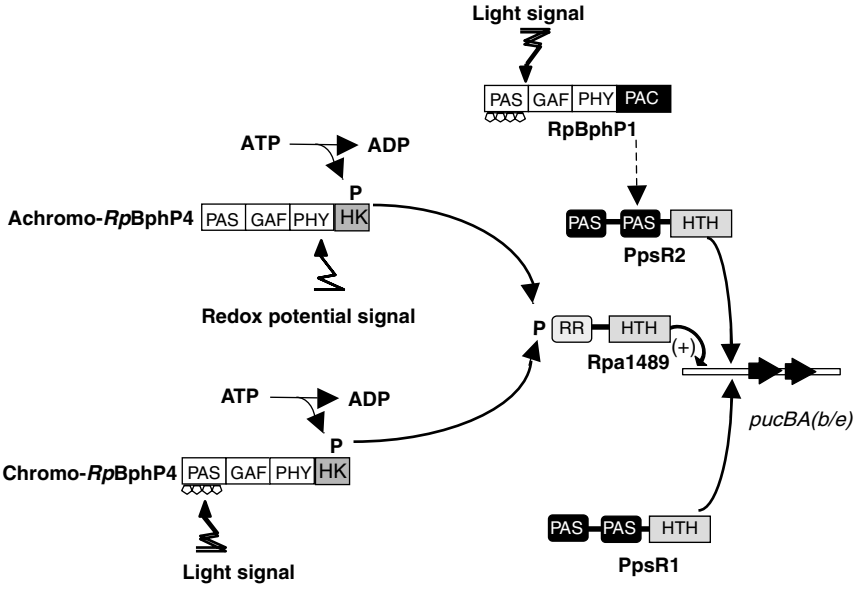

Figure 7 Proposed model for the regulation of LH2 antennae synthesis in *Rps. palustris*.

Materials and methods

Bacterial strains and growth conditions

Ten different strains of *Rps. palustris* were used: the CEA001 strain (Giraud *et al*, 2004); the CGA009, HaA2 and BisB5 strains (kindly provided by Dr Harwood, Department of Microbiology, University of Iowa, USA); the DSM126, DSM131, DSM7375 and DSM8283 strains (purchased from the DSMZ Collection) and the LMG4316 and LMG4317 strains (purchased from the BCCM/LMG Bacteria Collection). Cells were grown in liquid medium under different light or oxygen conditions, as previously described (Giraud *et al*, 2004). Light was provided by light-emitting diodes emitting at 700 or 770 nm (ELD700-524 and ELD 770-524 from Roithner), with an irradiance of 200 and 100 μmol of photon/m^2/s, respectively.

Isolation of RpBphP4 and sequencing

The *RpBphP4* gene from different *Rps. palustris* strains was amplified by PCR, using the following primers: *pucB.e.f* (5′-CAACGACGAGTCGCCTCGCGTTG-3′)/*rpa1489.r* (5′-AGCGCCTTC ATGCCGCTGAGCAC-3′). The sequences of the PCR products have been submitted to the GenBank databases under the following accession numbers (CEA001, EF010855; LMG4317, EF010856; DSM126, EF010857; DSM8283, EF010858; DSM7375, EF010859; LMG4316, EF01860; DSM131, EF010861).

Expression and protein procedures

The *RpBphP4* gene was amplified by PCR from *Rps. palustris* genomic DNA from the CEA001, HaA2 and Bis5 strains and the *rpa1489* gene from CEA001. Primers designed to add appropriate restriction sites for expression as His_6-tagged versions in the pBAD/HisB expression vector (Invitrogen) were used. In order to reconstitute *Rp*BphP4 holobacteriophytochromes *in vivo*, the *hmuO* gene from *Bradyrhizobium* ORS278 was inserted in the above pBAD::*RpBphP4* constructs (described in Giraud *et al*, 2004). The recombinant proteins were overexpressed in *E. coli* LMG194 and purified, as previously described (Giraud *et al*, 2004). To test the reduction/oxidation of *Rp*BphP4 proteins, reducing conditions were created with 1 mM DTT and oxidizing conditions with 1 mM $K_3Fe(CN)_6$. After addition of the oxidizing or reducing reagents, the protein samples were incubated for at least 30 min on ice and then analyzed by non-reducing SDS–PAGE.

Site-directed mutagenesis

Single or double mutations were introduced into the achromo-*Rp*BphP4 protein from CEA001 using the QuickChange(tm) site-directed mutagenesis kit (Stratagene), according to the manufacturer's recommendations. To construct the achromo-*Rp*BphP4 C472S and C722S mutants, the plasmid pBAD::*RpBphP4* from CEA001 was used as the template with the following primer pairs: *Rp*BphP4-C472Ssens (5′-GAACGCCGAAAGGCAGCGCGTCGAGCT GG-3′)/BphP4-C472Santisens (5′-CCAGCTCGACGCGCTGCCTTTCG GCGTTC-3′) and BphP4-C722Ssens (5′-CGAGGATGACGGCTCA GGCTTCGTCACCG-3′)/BphP4-C722Santisens (5′-CGGTGACGAAGC CTGAGCCGTCATCCTCG-3′). To construct the double mutant, the pBAD::*RpBphP4-C472* plasmid was used as the template with the BphP4-C722Ssens/BphP4-C722Santisens primer pair.

Sulfhydryl alkylation

To alkylate protein thiol groups, purified achromo-*Rp*BphP4 was treated with 10 mM DTT for 30 min. DTT was removed from the sample on a desalting column and the reduced achromo-*Rp*BphP4 was then incubated at room temperature in the presence of 10 mM iodoacetamide for 3 h. Finally the alkylated sample was thoroughly dialyzed against 20 mM Tris–HCl (pH 8), 50 mM NaCl.

Gel mobility shift assay and DNase I footprint

Five probes corresponding to the *pucBA* promoter regions identified in *Rps. palustris* CGA009 were prepared by PCR using ^{32}P 5′-end-labeled oligonucleotide primers, as previously described (Giraud *et al*, 2004). For gel mobility shift assays, the purified Rpa1489 protein (0.5 μM) was added to 20 μl of reaction buffer composed of 5 fmol of ^{32}P-labeled DNA probe, 1 μg of polydIdC as competitor, 50 mM Tris–HCl (pH 8), 1 mM DTT, 50 mM potassium acetate, 5 μg of bovine serum albumin and 10% glycerol. The reaction mixture was incubated at room temperature for 30 min and was subjected to non-denaturing 5% Tris–glycine–EDTA-buffered polyacrylamide gel electrophoresis at 4°C for 4 h at 70 V. DNase I footprint experiments were performed as previously described (Giraud *et al*, 2004).

Protein kinase assays

Protein kinase reactions were performed as previously described (Giraud *et al*, 2005). For the phosphotransfer experiments, achromo- and chromo-*Rp*BphP4 were phosphorylated for 15 min in the presence of γ-^{32}P-ATP, under reducing conditions or following a 705 nm illumination, respectively. This phosphorylation step was followed by a 25 min incubation in the presence of a stoichiometric amount of Rpa1489. ^{32}P-labeled products were quantified with a Typhoon Phosphor-Imager (Amersham Biosciences).

Construction of RpBphP4 mutants

To create *RpBphP4*-null mutants for strains HaA2 (*RpBphP4.HaA2*) and BisB5 (*RpBphP4.BisB5*), a fragment of each gene was deleted (0.35 kb *Bam*HI for *RpBphP4.HaA2* and 50 bp *Sal*I for *RpBphP4.BisB5*) and replaced by the *lac*Z-Km^r cassette of pKOK5 (Kokotek and Lotz, 1989). The *RpBphP4.CEA001*-null mutant was obtained by inserting the *lac*Z-Km^r cassette directly into the unique *Bam*HI site of the *RpBphP4.CEA001* gene. These constructs were introduced into the pJQ200 suicide vector (Quandt and Hynes, 1993) and delivered by conjugation into the corresponding *Rps. palustris* strains, as described (Giraud *et al*, 2004). Double recombinants were selected on sucrose and confirmed by PCR.

Absorbance and fluorescence measurements

Absorbance and fluorescence spectra of purified chromo-*Rp*BphP4 from HaA2 and BisB5 were recorded as previously described (Giraud *et al*, 2005). Excitation was provided by light-emitting diodes emitting at 770 or 705 nm (ELD770-524 and ELD 700-524 from Roithner), with an irradiance of 15 μmol of photon/m^2/s.

Supplementary data

Supplementary data are available at *The EMBO Journal* Online (http://www.embojournal.org).

Acknowledgements

We thank Professor C Harwood (University of Iowa, USA) for the generous gift of the CGA009, HaA2 and BisB5 strains. LV is indebted to the French Ministry of National Education, Higher Education and Research for a doctoral grant.

References

Bhoo SH, Davis SJ, Walker J, Karniol B, Vierstra RD (2001) Bacteriophytochromes are photochromic histidine kinases using a biliverdin chromophore. *Nature* **414:** 776–779

Borucki B, von Stetten D, Seibeck S, Lamparter T, Michael N, Mroginski MA, Otto H, Murgida DH, Heyn MP, Hildebrandt P (2005) Light-induced proton release of phytochrome is coupled to the transient deprotonation of the tetrapyrrole chromophore. *J Biol Chem* **280:** 34358–34364

Butler WL, Lane HC (1965) Dark transformations of phytochromes *in vivo*. II. *Plant Physiol* **40:** 13–17

Eilfeld P, Rüdiger W (1985) Absorption spectra of phytochrome intermediates. *Z Naturforsch* **40C:** 109–114

Elsen S, Jaubert M, Pignol D, Giraud E (2005) PpsR: a multifaceted regulator of photosynthesis gene expression in purple bacteria. *Mol Microbiol* **57:** 17–26

Elsen S, Swem LR, Swem DL, Bauer CE (2004) RegB/RegA, a highly conserved redox-responding global two-component regulatory system. *Microbiol Mol Biol R* **68:** 263–279

Evans K, Fordham-Skelton AP, Mistry H, Reynolds CD, Lawless AM, Papiz MZ (2005) A bacteriophytochrome regulates the synthesis of LH4 complexes in *Rhodopseudomonas palustris*. *Photosynth Res* **85:** 169–180

Evans K, Grossmann G, Fordham-Skelton AP, Papiz MZ (2006) Small-angle X-ray scattering reveals the solution structure of a

bacteriophytochrome in the catalytically active Pr state. *J Mol Biol* **364:** 655–666

Evans MB, Hawthornthwaite AM, Cogdell RJ (1990) Isolation and characterisation of different B800-850 light-harvesting complexes from low-and high-light grown cells of *Rhodopseudomonas palustris*, strain 2.1.6. *Biochim Biophys Acta* **1016:** 71–76

Giraud E, Fardoux J, Fourrier N, Hannibal L, Genty B, Bouyer P, Dreyfus B, Verméglio A (2002) Bacteriophytochrome controls photosystem synthesis in anoxygenic bacteria. *Nature* **417:** 202–205

Giraud E, Zappa S, Jaubert M, Hannibal L, Fardoux J, Adriano J-M, Bouyer P, Genty B, Pignol D, Verméglio A (2004) Bacteriophytochrome and regulation of the synthesis of the photosynthetic apparatus in *Rhodopseudomonas palustris*: pitfalls of using laboratory strains. *Photochem Photobiol Sci* **3:** 587–591

Giraud E, Zappa S, Vuillet L, Adriano J-M, Hannibal L, Fardoux J, Berthomieu C, Bouyer P, Pignol D, Verméglio A (2005) A new type of bacteriophytochrome acts in tandem with a classical bacteriophytochrome to control the antennae synthesis in *Rhodopseudomonas palustris*. *J Biol Chem* **280:** 32389–32397

Hartigan N, Tharia HA, Sweeney F, Lawless AM, Papiz MZ (2002) The 7.5-Å electron density and spectroscopic properties of a novel low-light B800 LH2 from *Rhodopseudomonas palustris*. *Biophys J* **82:** 963–977

Jaubert M, Lavergne J, Fardoux J, Hannibal L, Vuillet L, Adriano J-M, Bouyer P, Pignol D, Giraud E, Verméglio A (2007) A singular bacteriophytchrome acquired by lateral gene transfer. *J Biol Chem* **282:** 7320–7328

Jaubert M, Zappa S, Fardoux J, Adriano J-M, Hannibal L, Elsen S, Lavergne J, Verméglio A, Giraud E, Pignol D (2004) Light and redox control of photosynthesis gene expression in *Bradyrhizobium*: dual roles of two PpsR. *J Biol Chem* **279:** 44407–44416

Jiang ZY, Swem LR, Rushing BG, Devanathan S, Tollin G, Bauer CE (1999) Bacterial photoreceptor with similarity to photoactive yellow protein and plant phytochromes. *Science* **285:** 406–409

Karniol B, Viestra RD (2003) The pair of bacteriophytochromes from *Agrobacterium tumefaciens* are histidine kinases with opposing photobiological properties. *Proc Natl Acad Sci USA* **100:** 2807–2812

Karniol B, Wagner JR, Walker JM, Vierstra RD (2005) Phylogenetic analysis of the phytochrome superfamily reveals distinct microbial subfamilies of photoreceptors. *Biochem J* **392:** 103–116

Kokotek W, Lotz W (1989) Construction of a *lacZ*-kanamycine–resistance cassette, useful for site-directed mutagenesis and as a promoter probe. *Gene* **84:** 467–471

Lamparter T, Michael N, Mittmann F, Esteban B (2002) Phytochrome from *Agrobacterium tumefaciens* has unusual spectral properties and reveals an N-terminal chromophore attachment site. *Proc Natl Acad Sci USA* **99:** 11628–11633

Larimer FW, Chain P, Hauser L, Lamerdin J, Malfatti S, Do L, Land ML, Pelletier DA, Beatty JT, Lang AS, Tabita FR, Gibson JL, Hanson TE, Bobst C, Torres JL, Peres C, Harrison FH, Gibson J, Harwood CS (2004) Complete genome sequence of the metabolically versatile photosynthetic bacterium *Rhodopseudomonas palustris*. *Nat Biotech* **22:** 55–61

Masuda S, Dong C, Swem D, Setterdahl AT, Knaff DB, Bauer CE (2002) Repression of photosynthesis gene expression by formation of a disulfide bond in CrtJ. *Proc Natl Acad Sci USA* **99:** 7078–7083

Ninfa EG, Atkinson MR, Kamberov ES, Ninfa AJ (1993) Mechanism of autophosphorylation of *Escherichia coli* nitrogen regulator II (NR_{II} or NtrB): trans-phosphorylation between subunits. *J Bacteriol* **175:** 7024–7032

Paget MS, Buttner MJ (2003) Thiol-based regulatory switches. *Annu Rev Genet* **37:** 91–121

Quandt J, Hynes MF (1993) Versatile suicide vectors which allow direct selection for gene replacement in gram-negative bacteria. *Gene* **127:** 15–21

Rockwell NC, Su YS, Lagarias JC (2006) Phytochrome structure and signaling mechanisms. *Annu Rev Plant Biol* **57:** 837–858

Swem LR, Kraft BJ, Swem DL, Setterdahl AT, Masuda S, Knaff DB, Zaleski JM, Bauer CE (2003) Signal transduction by the global regulator RegB is mediated by a redox-active cysteine. *EMBO J* **22:** 4699–4708

Tadros MH, Waterkamp K (1989) Multiple copies of the coding regions for the light-harvesting B800-850 alpha- and beta-polypeptides are present in the *Rhodopseudomonas palustris* genome. *EMBO J* **8:** 1303–1308

Wagner JR, Brunzelle JS, Forest KT, Vierstra RD (2005) A light-sensing knot revealed by the structure of the chromophore-binding domain of phytochrome. *Nature* **438:** 325–331

Yang Y, Inouye M (1991) Intermolecular complementation between two defective mutant signal-transducing receptors of *Escherichia coli*. *Proc Natl Acad Sci USA* **88:** 11057–11061